catalysts

MDPI

Article

Substrate Specificity of an Aminopropyltransferase and the Biosynthesis Pathway of Polyamines in the Hyperthermophilic Crenarchaeon *Pyrobaculum calidifontis*

Wakao Fukuda [1,2,*], Mamoru Osaki [1], Yusuke Yasuda [3], Ryota Hidese [4], Tsunehiko Higuchi [5], Naoki Umezawa [5], Shinsuke Fujiwara [1,2] and Eiichi Mizohata [3,6,*]

1 Department of Bioscience, Graduate School of Science and Technology, Kwansei-Gakuin University, 1 Gakuen Uegahara, Sanda 669-1330, Hyogo, Japan; garder.def.331@gmail.com (M.O.); fujiwara-s@kwansei.ac.jp (S.F.)
2 Department of Biosciences, School of Biological and Environmental Sciences, Kwansei-Gakuin University, 1 Gakuen Uegahara, Sanda 669-1330, Hyogo, Japan
3 Department of Applied Chemistry, Graduate School of Engineering, Osaka University, 2-1 Yamadaoka, Suita 565-0871, Osaka, Japan; yuxile7@gmail.com
4 Graduate School of Science, Technology and Innovation, Kobe University, 1-1 Rokkodai, Nada, Kobe 657-8501, Hyogo, Japan; hidese@people.kobe-u.ac.jp
5 Graduate School of Pharmaceutical Sciences, Nagoya City University, 3-1, Tanabe-dori, Mizuho-ku, Nagoya 467-8603, Aichi, Japan; higuchi@phar.nagoya-cu.ac.jp (T.H.); umezawa@phar.nagoya-cu.ac.jp (N.U.)
6 Japan Science and Technology Agency, PRESTO, Kawaguchi 332-0012, Saitama, Japan
* Correspondence: wfukuda@kwansei.ac.jp (W.F.); mizohata@chem.eng.osaka-u.ac.jp (E.M.); Tel.: +81-79-565-7829 (W.F.); +81-6-6879-7410 (E.M.); Fax: +81-79-565-9077 (W.F.); +81-6-6879-7409 (E.M.)

check for updates

Citation: Fukuda, W.; Osaki, M.; Yasuda, Y.; Hidese, R.; Higuchi, T.; Umezawa, N.; Fujiwara, S.; Mizohata, E. Substrate Specificity of an Aminopropyltransferase and the Biosynthesis Pathway of Polyamines in the Hyperthermophilic Crenarchaeon *Pyrobaculum calidifontis*. *Catalysts* **2022**, *12*, 567. https://doi.org/10.3390/catal12050567

Academic Editors: Giuseppe Perugino, Isaac Cann, Anna Valenti and Cinzia Verde

Received: 3 May 2022
Accepted: 19 May 2022
Published: 20 May 2022

Abstract: The facultative anaerobic hyperthermophilic crenarchaeon *Pyrobaculum calidifontis* possesses norspermine (**333**), norspermidine (**33**), and spermidine (**34**) as intracellular polyamines (where the number in parentheses represents the number of methylene CH_2 chain units between NH_2, or NH). In this study, the polyamine biosynthesis pathway of *P. calidifontis* was predicted on the basis of the enzymatic properties and crystal structures of an aminopropyltransferase from *P. calidifontis* (*Pc*-SpeE). *Pc*-SpeE shared 75% amino acid identity with the thermospermine synthase from *Pyrobaculum aerophilum*, and recombinant *Pc*-SpeE could synthesize both thermospermine (**334**) and spermine (**343**) from spermidine and decarboxylated *S*-adenosyl methionine (dcSAM). Recombinant *Pc*-SpeE showed high enzymatic activity when aminopropylagmatine and norspermidine were used as substrates. By comparison, *Pc*-SpeE showed low affinity toward putrescine, and putrescine was not stably bound in its active site. Norspermidine was produced from thermospermine by oxidative degradation using a cell-free extract of *P. calidifontis*, whereas 1,3-diaminopropane (**3**) formation was not detected. These results suggest that thermospermine was mainly produced from arginine via agmatine, aminopropylagmatine, and spermidine. Norspermidine was produced from thermospermine by an unknown polyamine oxidase/dehydrogenase followed by norspermine formation by *Pc*-SpeE.

Keywords: polyamine; crenarchaeota; biosynthetic pathway; X-ray crystallography; structure–function relationship; dcSAM

1. Introduction

Polyamines are organic polycations that have two or more primary amines and modulate various cellular processes in many living organisms, including transcription and translation, cell proliferation, cell differentiation, and adaptation to various stresses. Putrescine (**4**), spermidine (**34**), and spermine (**343**) (where the number in parentheses represents the number of methylene CH_2 chain units between NH_2, or NH) are common polyamines that are found in a variety of organisms. Polyamines are synthesized from arginine or ornithine, and aminopropyl groups from decarboxylated *S*-adenosyl methionine (dcSAM)

are added for the synthesis of larger polyamines (Figure 1). Therefore, polyamines usually consist of one putrescine unit and zero to two aminopropyl groups. In some eucaryotes, polyamine oxidases catalyze the oxidation of the free and/or acetylated form of polyamines at the secondary amino groups. For example, in the case of *Arabidopsis thaliana*, some enzymes catalyze oxidative degradation from N^1-acetylspermidine to putrescine and 3-acetamidopropanal, and others catalyze oxidative degradation from spermidine to putrescine and 3-aminobutanal. It is known that 1,3-diaminopropane (**3**) is produced by oxidative degradation of spermidine catalyzed by polyamine oxidase in eucaryotes via acetylated spermidine [1,2]. In some bacterial species, such as *Pseudomonas aeruginosa*, FAD-dependent spermidine dehydrogenases, which prefer potassium ferricyanide as an electron acceptor, yielded mostly 1,3-diaminopropane (**3**) and 4-aminobutyraldehyde from spermidine [3]. In addition to common polyamines, (hyper)thermophilic euryarchaea and bacteria possess long-chain and/or branched-chain polyamines (BCPAs), which are especially important for the growth of thermophiles at high temperatures [4–7]. By comparison, crenarchaea that live in a high-temperature environment do not produce BCPAs; instead, linear-chain polyamines are detected [8]. It is an interesting fact that hyperthermophilic crenarchaea can grow at extreme condition without the help of large polyamines for stabilization of biological molecules, such as RNA, DNA, and protein. Furthermore, the polyamine metabolisms in crenarchaea have been still unclear, as described below.

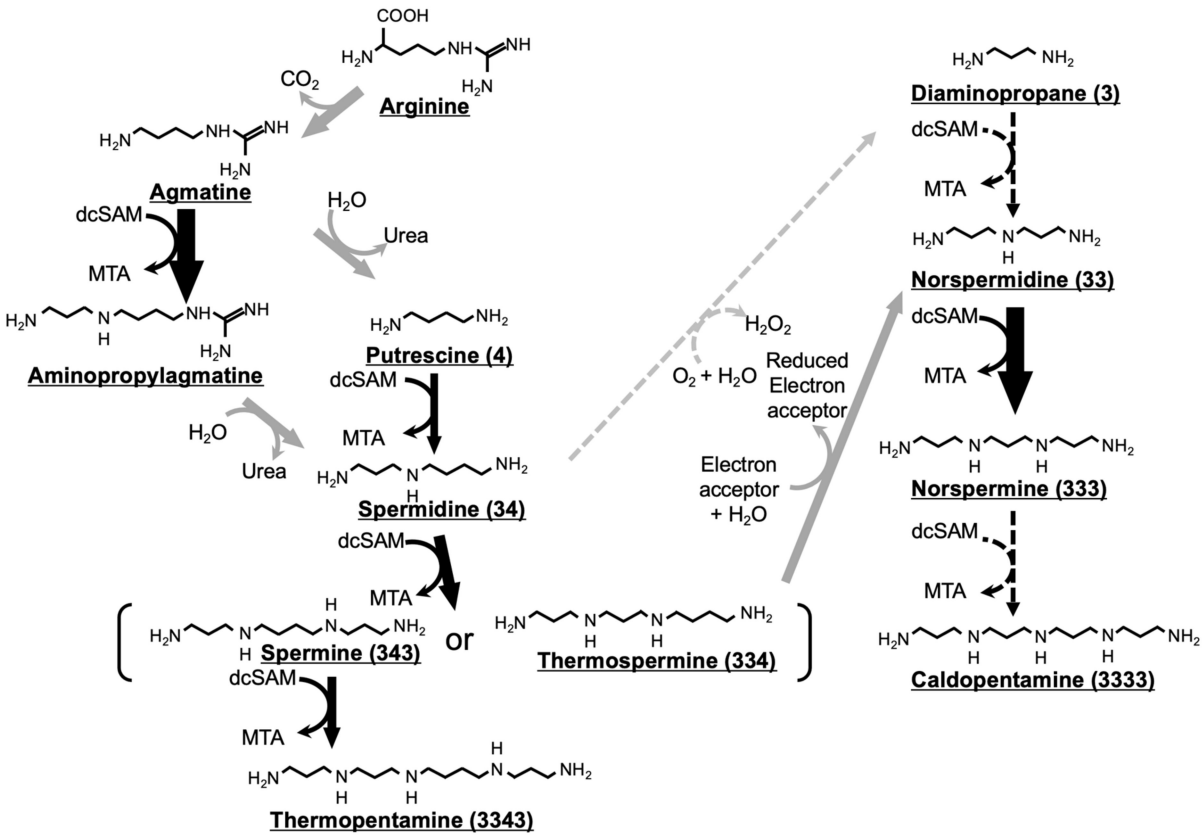

Figure 1. The predicted polyamine biosynthesis pathway in *Pyrobaculum calidifontis*. Black arrows indicate the reactions catalyzed by an aminopropyltransferase (*Pc*-SpeE). Gray arrows indicate the reactions that are not catalyzed by an aminopropyltransferase. Dashed lines indicate the reactions that are unlikely to occur in *P. calidifontis* based on the results from this study. The number in parentheses represents the number of methylene CH_2 chain units between NH_2, or NH.

The facultative anaerobic hyperthermophilic crenarchaeon *Pyrobaculum calidifontis* was isolated from a terrestrial hot spring in the Philippines [9]. It grows optimally at 90 to 95 °C [10]. *P. calidifontis* produces mainly norspermidine (**33**), spermidine (**34**), and

norspermine (**333**) [8]. Crenarchaeota possesses arginine decarboxylase, which is homologous to *S*-adenosylmethionine decarboxylase [11]. *P. calidifontis* possesses two homologues of *S*-adenosylmethionine decarboxylase (Pcal_0636 and Pcal_0807), which contribute to the decarboxylation of arginine and *S*-adenosylmethionine for polyamine biosynthesis. Additionally, genes coding an agmatinase homologue (Pcal_1626) and an aminopropyltransferase homologue (*Pc*-SpeE, Pcal_0772) have been identified on the genome of *P. calidifontis*. *Pc*-SpeE is expected to contribute to the elongation of some polyamines, but the details are unclear. Although a polyamine oxidase has not been identified in the genome of *P. calidifontis*, the presence of norspermidine and norspermine in a cell-free extract suggests that oxidative degradation of polyamine, which produces 1,3-diaminopropane as a coproduct, is expected to occur in *P. calidifontis* (Figure 1). In this study, to clarify the polyamine biosynthetic pathway of the hyperthermophilic crenarchaeon *P. calidifontis*, the enzymatic characteristics of *Pc*-SpeE were analyzed. Furthermore, crystal structures of *Pc*-SpeE with substrates were solved to clarify the substrate specificities of *Pc*-SpeE. In addition, the polyamine oxidase activity in the cell-free extract was confirmed.

2. Experimental Procedures

2.1. Strains, Culture Conditions, and Polyamine Composition

P. calidifontis strain JCM11548^T (=VA1^T) was cultivated under aerobic conditions at 90 °C in a medium containing the following components (per liter): 10 g tryptone, 1 g yeast extract, and 3 g $Na_2S_2O_3 \cdot 5H_2O$. Samples were grown in an air bath shaker (120 rpm), as described previously [10]. For the anaerobic cultivation, resazurin sodium salt (0.5 mg/L) was added as an oxygen indicator and 5.0% $Na_2S \cdot 9H_2O$ was added until the medium became colorless. *Escherichia coli* DH5α was used to maintain and amplify the plasmid. *E. coli* BL21-CodonPlus(DE3)-RIL (Agilent Technologies, Santa Clara, CA, USA) and pET28a (Merck KGaA, Darmstadt, Germany) were used for gene expression. *E. coli* strains were routinely cultivated at 37 °C in a Luria–Bertani (LB) medium. Ampicillin (50 μg/mL) and/or chloramphenicol (25 μg/mL) were added to the medium when needed. The polyamine composition was analyzed as described previously [4].

2.2. DNA Manipulation and Sequencing

DNA manipulations were carried out by standard techniques, as described previously by Sambrook and Russell [12]. Restriction enzymes and other modifying enzymes were purchased from Takara (Takara, Kyoto, Japan) or Toyobo (Toyobo, Osaka, Japan). Plasmid DNA was isolated with a Wizard Plus Minipreps DNA Purification System (Promega, Tokyo, Japan). A FastGene Gel/PCR Extraction Kit (Nippon Genetics, Tokyo, Japan) was used to recover the DNA fragments from the agarose gels after electrophoresis. DNA sequencing was performed with a BigDye-Terminator cycle-sequencing ready reaction kit, Version 3.1, and a model 3130 capillary DNA sequencer (Applied Biosystems, Tokyo, Japan).

2.3. Expression and Purification of Pc-SpeE

The expression plasmid for pET-PcSpeE was constructed as follows. The *Pc-SpeE* (PCAL_RS04120) was amplified with *P. calidifontis* genomic DNA as the template and two oligonucleotide primers (sense, 5′-AAAAAAACATATGCGCAAGGTGCCCGGTCC-3′; antisense, 5′-AGAATTCTCATCTGAGTTTTCTGTGTA-3′ (underlined sequences indicate the NdeI and EcoRI sites in the sense and antisense primers, respectively)). The amplified fragments were inserted into pET28a and the constructed plasmid was designated as pET-PcSpeE. After confirming the absence of unintended mutations in the fragment, pET-PcSpeE was used to transform *E. coli* BL21-CodonPlus(DE3)-RIL. The recombinant cells were cultivated until the OD_{660} reached 0.6. After induction with 1 mM isopropyl-β-D-thiogalactopyranoside for 4 h, cells were harvested by centrifugation (6000× *g* for 20 min at 4 °C) and resuspended in 20 mM Tris-HCl buffer (pH 7.5) containing 1 mM EDTA, 0.2 mM PMSF, and 1 mM 2-mercaptoethanol. After sonication, the supernatant was obtained by centrifugation (8000× *g* for 20 min at 4 °C). The supernatant was incubated at 85 °C for

20 min and centrifuged (16,100× *g* for 30 min at 4 °C) again. The supernatant was applied to an anion exchange column HiTrapQ HP (Cytiva, Marlborough, MA, USA) with a mobile phase of 20 mM Tris-HCl buffer (pH 8.0) and eluted with a linear gradient of 0 to 1000 mM NaCl. To calibrate the molecular mass of the subunits of *Pc*-SpeE, the recombinant *Pc*-SpeE was subjected to gel-filtration chromatography using a Superdex-200 HR 10/30 column (Cytiva) with a mobile phase of 20 mM Tris-HCl buffer (pH 8.0) containing 150 mM NaCl. The protein concentration was determined using a Coomassie Plus Protein Assay Reagent Kit (Pierce, Rockford, IL, USA) according to the manufacturer's instructions using bovine serum albumin as a standard.

2.4. Enzymatic Assay Condition of Pc-SpeE

Recombinant *Pc*-SpeE was added to a reaction mixture containing 20 mM PIPES-NaOH (pH 8.5), 0.5 mM dcSAM, 0.5 µg *Pc*-SpeE, and polyamines as acceptors of the aminopropyl group. The reaction mixture was incubated at 90 °C for 6 min. After the reaction, the polyamine composition was analyzed by HPLC as described previously [4]. The structures of the polyamines were analyzed by GC–MS using a JMS-700 (JEOL, Tokyo, Japan) equipped with an inertCap 1MS column (0.32 mm i.d. × 30 m coiled column; GL Sciences, Tokyo, Japan).

2.5. X-ray Crystallography of Pc-SpeE

Pc-SpeE−ligand complexes were prepared by incubating the protein solution (10 mg/mL *Pc*-SpeE, 20 mM Tris-HCl buffer pH 8.0, 150 mM NaCl) with 4 mM dcSAM and 2 mM polyamine (putrescine, spermidine, spermine or aminopropylagmatine) at 20 °C for 1 h. Crystallization was performed using the sitting-drop vapor diffusion method in a drop containing a 1:1 mixture of the protein−ligand solution to the mother liquor solution (Table 1).

Table 1. Mother liquor solution for the crystallization of *Pc*-SpeE.

Donor	Acceptor	Composition of Mother Liquor Solution
dcSAM	Putrescine	0.4 M Ammonium acetate pH 8.0, 16% (*w*/*v*) PEG 2000MME
	Spermidine	0.34 M Ammonium sulfate, 0.1 M Sodium citrate pH 5.2, 11% (*w*/*v*) PEG 4000
	Spermine	0.15 M Sodium formate, 0.1 M HEPES pH 7.2, 18% (*w*/*v*) PEG 3350
	Agmatine	0.15 M Sodium formate, 0.1 M HEPES pH 6.8, 15% (*w*/*v*) PEG 3350

Donor, donor substrate of aminopropyl group; Acceptor, acceptor substrate of aminopropyl group (polyamine).

Each obtained crystal was soaked in cryoprotectant solution (mother liquor solution supplemented with 30% *v*/*v* glycerol), fished with a cryo-loop, and frozen in liquid N_2. X-ray diffraction data were collected at the SPring-8 BL44XU beamline at 100 K. Datasets were processed using *XDS* [13] and the *CCP4* suite (ver. 7.1.016) [14]. First, the structure of *Pc*-SpeE incubated with dcSAM and spermidine was determined by the molecular replacement method with *MOLREP* [15] using the structure of aminopropyltransferase from *Thermus thermophilus* (*Tth*-SpeE; Protein Data Bank (PDB) ID: 3ANX) as the search model. Using this structure as the search model, the other structures were solved by the molecular replacement method. The structures were iteratively refined with *REFMAC* [16], while manual model building was performed using the molecular graphics program *COOT* [17]. All protein figures were generated using *PyMOL* (https://www.pymol.org accessed on 2 May 2022). Data collection and refinement statistics for the final coordinates are given in Table 2. The final coordinates and structure factor amplitudes were deposited to the PDB with IDs 7XIF for the complex of 5′-methylthioadenosine (MTA) alone or together with spermidine or thermospermine (**334**), 7XIG for the complex of MTA and

spermine, 7XIH for the complex of MTA and spermidine, and 7XII for the complex of MTA and aminopropylagmatine.

Table 2. Crystallographic data collection and refinement statistics of *Pc*-SpeE.

PDB IDs	7XIF	7XIG	7XIH	7XII
Substrates added in crystallization conditions	dcSAM and spermidine	dcSAM and spermine	dcSAM and putrescine	dcSAM and agmatine
Ligands observed in catalytic pockets	MTA alone or together with spermidine or thermospermine	MTA and spermine	MTA and spermidine	MTA and aminopropylagmatine
Data collection				
Synchrotron beamline	SPring-8 BL44XU	SPring-8 BL44XU	SPring-8 BL44XU	SPring-8 BL44XU
No. of measured crystal(s)	1	2	1	3
Wavelength (Å)	0.90000	0.90000	0.90000	0.90000
Space group	$P3_1$	$P1$	$C2$	$P1$
Unit cell a, b, c (Å)	166.16, 166.16, 149.59	77.83, 80.39, 97.84 72.46,	176.57, 57.26, 54.49	55.16, 57.17, 97.31 77.19,
α, β, γ (°)	90.00, 90.00, 120.00	89.13, 88.08	90.00, 98.50, 90.00	78.32, 88.49
Resolution range (Å)	47.97–2.14 (2.18–2.14)	46.65–2.25 (2.29–2.25)	43.10–1.20 (1.22–1.20)	46.47–2.25 (2.32–2.25)
Completeness (%)	99.8 (100.0)	99.5 (97.6)	99.2 (99.7)	99.5 (96.1)
No. of total reflections	1118,232	379,621	557,761	531,582
No. of unique reflections	254,276 (12,626)	106,737 (5243)	166,200 (8259)	53,669 (4661)
Redundancy	4.4 (4.5)	3.6 (3.1)	3.4 (3.4)	9.9 (9.8)
R_{merge} (all I+ and I−) (%)	6.5 (95.2)	13.8 (391.9)	3.4 (70.5)	14.5 (41.8)
$<I/<\sigma(I)>$	15.2 (1.7)	5.4 (1.2)	15.1 (2.1)	13.3 (7.5)
$CC_{1/2}$	0.999 (0.526)	0.989 (0.813)	0.999 (0.778)	0.995 (0.961)
Refinement				
Resolution range (Å)	47.11–2.14	46.69–2.25	39.23–1.20	46.51–2.25
No. of reflections	241,370	100,802	158,009	51,035
R_{work}/R_{free} (%)	16.0/19.0	17.3/20.7	11.9/15.4	14.9/17.0
Mean B value (Å^2)	46.2	47.3	21.4	24.4
No. of non-H atoms	28,933	19,343	5290	9834
RMSD from ideal bond length (Å)/angle (°)	0.011/1.597	0.007/1.467	0.017/2.045	0.010/1.684
Ramachandran (%)				
Favored	95.70	96.14	97.07	96.32
Allowed	3.59	3.51	2.56	3.16
Outliers	0.71	0.35	0.37	0.53

Values in parentheses are for the highest resolution shells.

2.6. Enzymatic Assay of Oxidative Polyamine Degradation

P. calidifontis was cultivated under aerobic or anaerobic conditions, and the harvested cells were disrupted. Polyamines (1 mM spermidine, spermine, thermospermine, or thermopentarmine (**3343**)) were added to a 200 µL reaction mixture containing 50 mM Tris-HCl (pH 7.5) buffer and the cell-free extract containing 10 µg protein. NAD^+, $NADP^+$, or potassium ferricyanide (1 mM each) were added to the reaction mixture when required. Then, the reaction mixture was incubated at 90 °C for 10 min, and the polyamine composition was analyzed by HPLC.

3. Results

3.1. Phylogenetic Analysis of Pc-SpeE

The facultative anaerobic hyperthermophilic archaeon *P. calidifontis* possesses mainly norspermidine, spermidine, and norspermine [8]. In this study, norspermine was detected as a major polyamine, and spermidine was detected as a minor polyamine of *P. calidifontis* (Figure 2A). In addition, small amounts of putrescine and norspermidine were detected. From the genome analysis, *Pc*-SpeE (Pcal_0772) was annotated as an aminopropyltransferase, and no other aminopropyltransferase homologue was identified. Therefore, *Pc*-SpeE was expected to contribute to the production of these linear polyamines found in *P. calidifontis* cells.

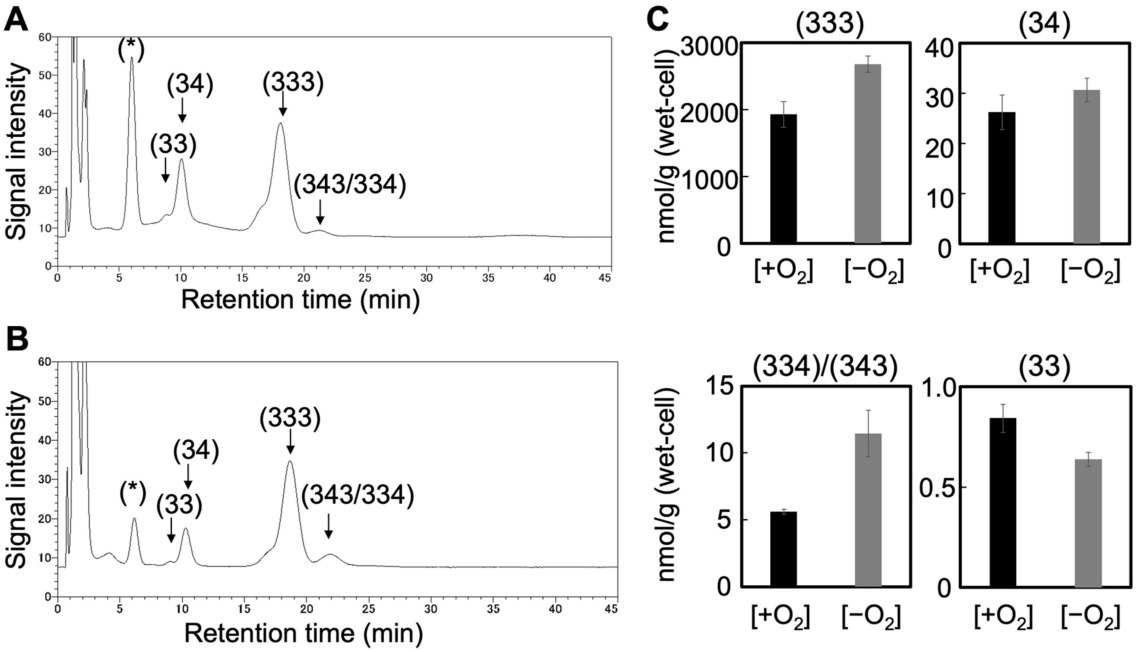

Figure 2. HPLC analysis of the intracellular polyamines of cells grown under (**A**) aerobic conditions and (**B**) anaerobic conditions. (**C**) Calculated intracellular polyamine (norspermine, norspermidine, spermidine, and spermine/thermospermine) concentrations of *P. calidifontis*. Asterisks (*) indicate the peak from an unknown compound. [+O_2] and [−O_2] indicate cells grown under aerobic and anaerobic conditions, respectively.

The amino acid sequence of *Pc*-SpeE shares 75% identity with that from *P. aerophilum* (*Pa*-SpeE), which produces norspermine and thermospermine [18]. When a phylogenetic tree was constructed based on the amino acid sequences of the aminopropyltransferases, the aminopropyltransferases were divided according to substrate specificity as described previously [4,19]. *Pc*-SpeE was located in the branch that included thermospermine synthases from crenarchaea (Figure 3). The thermospermine synthase from the hyperthermophilic crenarchaeon *Hyperthermus butylicus* (*Hb*-SpeEII), producing long-chain polyamines such as caldopentamine (**3333**), was located in the same branch [18]. In addition, the aminopropyltransferase from the thermophilic bacteria *T. thermophilus* (*Tth*-SpeE) was located in the same group. The branched-chain polyamine-producing enzymes, such as *Tk*-BpsA, were located in a distinct branch from *Pc*-SpeE [4]. By comparison, the aminopropylagmatine synthase from *Thermococcus kodakarensis* (TK0147) was located in a relatively close branch to that containing *Pc*-SpeE.

3.2. Enzymatic Properties

The molecular mass of the recombinant *Pc*-SpeE monomer containing a hexahistidine tag was theoretically calculated to be 34.8 kDa from the primary sequence, and the

apparent native molecular mass was estimated to be 134 kDa by gel-filtration chromatography, suggesting that *Pc*-SpeE is a homotetramer similar to the spermidine synthases from *T. thermophilus* and *Thermotoga maritima* [20,21]. When spermidine was used as a substrate for the enzymatic reaction of recombinant *Pc*-SpeE, both spermine (**343**) and thermospermine (**334**) were detected as enzymatic products by GC–MS analysis (data not shown). The signal intensity of thermospermine was higher than that of spermine. These results suggested that thermospermine was a major product of the enzymatic reaction of *Pc*-SpeE and spermidine. Next, the kinetic parameters of recombinant *Pc*-SpeE with various substrates were calculated (Table 3). The K_m values for agmatine and norspermidine were lower than those for spermidine. Additionally, *Pc*-SpeE showed high activities when agmatine and norspermidine were used as substrates. This result was consistent with the high activities observed for *Pa*-SpeE and *Hb*-SpeEII toward norspermidine [18]. Moreover, the high K_m and low V_{max} values obtained for the short-chain polyamines, such as 1,3-diaminopropane (**3**), suggested they were not applicable as substrates for the enzymatic reactions catalyzed by *Pc*-SpeE. The enzymatic properties of *Pc*-SpeE were different from those of *Pa*-SpeE and *Hb*-SpeEI, which showed relatively high activities toward 1,3-diaminopropane [18]. When putrescine at a high concentration was used as a substrate of *Pc*-SpeE, a relatively high V_{max} value was observed. By comparison, lower activity was observed when a low concentration of putrescine was used as a substrate. *Pa*-SpeE showed very low activity toward putrescine [18]. Considering the low affinity of *Pc*-SpeE to putrescine and its high affinity to agmatine, biosynthesis of spermidine via aminopropylagmatine seems to be the major polyamine biosynthetic pathway in *P. calidifontis* cells. The fact that 1,3-diaminopropane was hardly used as a substrate of *Pc*-SpeE suggested that norspermidine was not produced via 1,3-diaminopropane. The low K_m and high V_{max} values for the *Pc*-SpeE-catalyzed reaction of agmatine suggested that spermidine was produced via aminopropylagmatine similar to the polyamine biosynthesis carried out by the thermophilic bacteria *T. thermophilus* and the euryarchaeon *T. kodakarensis*.

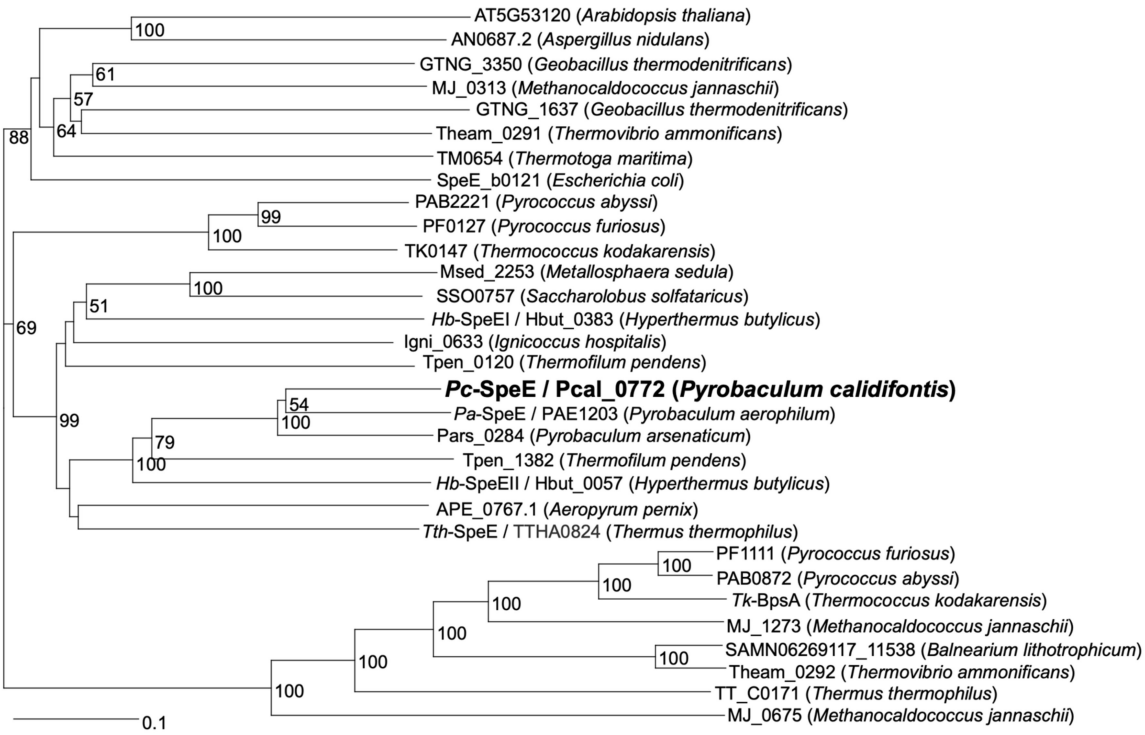

Figure 3. Phylogenetic tree of aminopropyltransferases involved in polyamine synthesis. *Pc*-SpeE is indicated in bold. Phylogenetic analysis was performed using the neighbor-joining method of the ClustalW program provided by DNA Data Bank of Japan. The scale bar represents one substitution per 10 amino acids. Bootstrap values of 50 to 100 trials are shown.

Table 3. Kinetic parameters of *Pc*-SpeE.

Substrate	K_m (μM)	V_{max} (Unit/mg)	k_{cat} (/s/Site)
Agmatine	54.4	1.00×10^3	0.580
1,3-diaminopropane	2.55×10^3	3.73	0.00216
Putrescine (0–1000 μM)	745	434	0.252
Putrescine (2000–3000 μM)	-	833	0.483
Norspermidine	33.7	769	0.446
Spermidine	99.5	40.7	0.0236
Norspermine	ND	ND	ND
Spermine	192	25.7	0.0149

One unit of activity was defined as the amount of enzyme that produces 1 nmol of product per min. The turnover number (k_{cat}) was calculated from V_{max} as a value per one second per one catalytic site. Abbreviations: -, not calculated; ND, not detectable.

3.3. X-ray Structural Analysis of Pc-SpeE Complexes

Four independent crystal structures with different ligand bindings were determined. These structures were determined from crystals obtained by co-crystallization of protein solutions mixed with various combinations of substrates under the sitting-drop vapor diffusion method. Crystallographic data collection and refinement statistics are summarized in Table 2. The results from all four structures showed that the subunit assembly of *Pc*-SpeE is a dimer of homodimers (homotetramer, 139.2 kDa) (Figure 4A), and the observed structure was consistent with the size estimated from gel-filtration chromatography as described above. Therefore, the results suggest that the biological assembly in the *P. calidifontis* cell is a dimer of homodimers. The assembly was the same as that of *Tth*-SpeE (PDB ID: 3ANX) [20,21] and thermospermine synthase from *Medicago truncatula* (6BQ2) [22], which shares 41% and 31% primary sequence identity, respectively, with *Pc*-SpeE, and was different from that of the aminopropyltransferase from *T. maritima* [20,21].

The crystal structure of *Pc*-SpeE in complex with MTA alone or together with spermidine or thermospermine was refined at 2.14 Å resolution. The crystal was obtained by co-crystallization of *Pc*-SpeE with dcSAM and spermidine. The asymmetric unit contained 12 *Pc*-SpeE monomers, of which four monomers were in the MTA alone complex without polyamine (*Pc*-SpeE/MTA), five monomers were in the MTA and spermidine complex (*Pc*-SpeE/MTA/spermidine), and three monomers were in the MTA and assigned thermospermine complex (*Pc*-SpeE/MTA/thermospermine) (Figure 4B). The fact that different complex structures were observed in the asymmetric unit indicates that the catalytic reaction occurred during crystallization and the products MTA and thermospermine (or spermine, which could be assigned in the electron density) were generated from the substrates dcSAM and spermidine, and the product thermospermine was released from some catalytic sites or exchanged with the new substrate spermidine.

The overall structure of *Pc*-SpeE is quite similar to that of *Tth*-SpeE, as indicated by the root mean square deviation (RMSD) value of 0.84 Å. The structure of the active site of the *Tth*-SpeE ternary complex had quite similar geometry to the *Pc*-SpeE ternary structure in that both active sites are surrounded by acidic residues, which accommodate the positively charged polyamine product, and the MTA-binding site is very close to the polyamine substrate-binding site. In the *Pc*-SpeE/MTA/thermospermine structure (Figure 4B), Ile^{56}, Asp^{167}, Asp^{164}, and Leu^{165} contributed to the stabilization of the polyamine by forming hydrogen bonds or salt bridges to the nitrogen atoms in thermospermine.

The *Pc*-SpeE complexed with MTA and spermine was obtained by co-crystallization of the protein with dcSAM and spermine, and the crystal structure (*Pc*-SpeE/MTA/spermine) was refined to 2.25 Å resolution (Figure 4C). The product thermopentamine from the substrate spermine was not observed in the catalytic pocket, possibly because the affinity for the product is much lower than that for the substrate, so the exchange of product and substrate occurred quickly. When the catalytic site structures of *Pc*-SpeE/MTA/thermospermine and *Pc*-SpeE/MTA/spermine were compared, it was noted that the interactions between the amino acid residues and polyamines were different. The hydrogen bond distance between

Asp[167] and the N8 atom of thermospermine (3.2 Å) was shorter than that between Asp[167] and the N4 atom of spermine (3.4 Å). The distance between the aromatic ring of Tyr[236] and the alkyl chain of thermospermine (3.4 Å) was shorter than that of spermine (4.4 Å). These differences in the hydrophilic and hydrophobic interactions may contribute to polyamine substrate recognition.

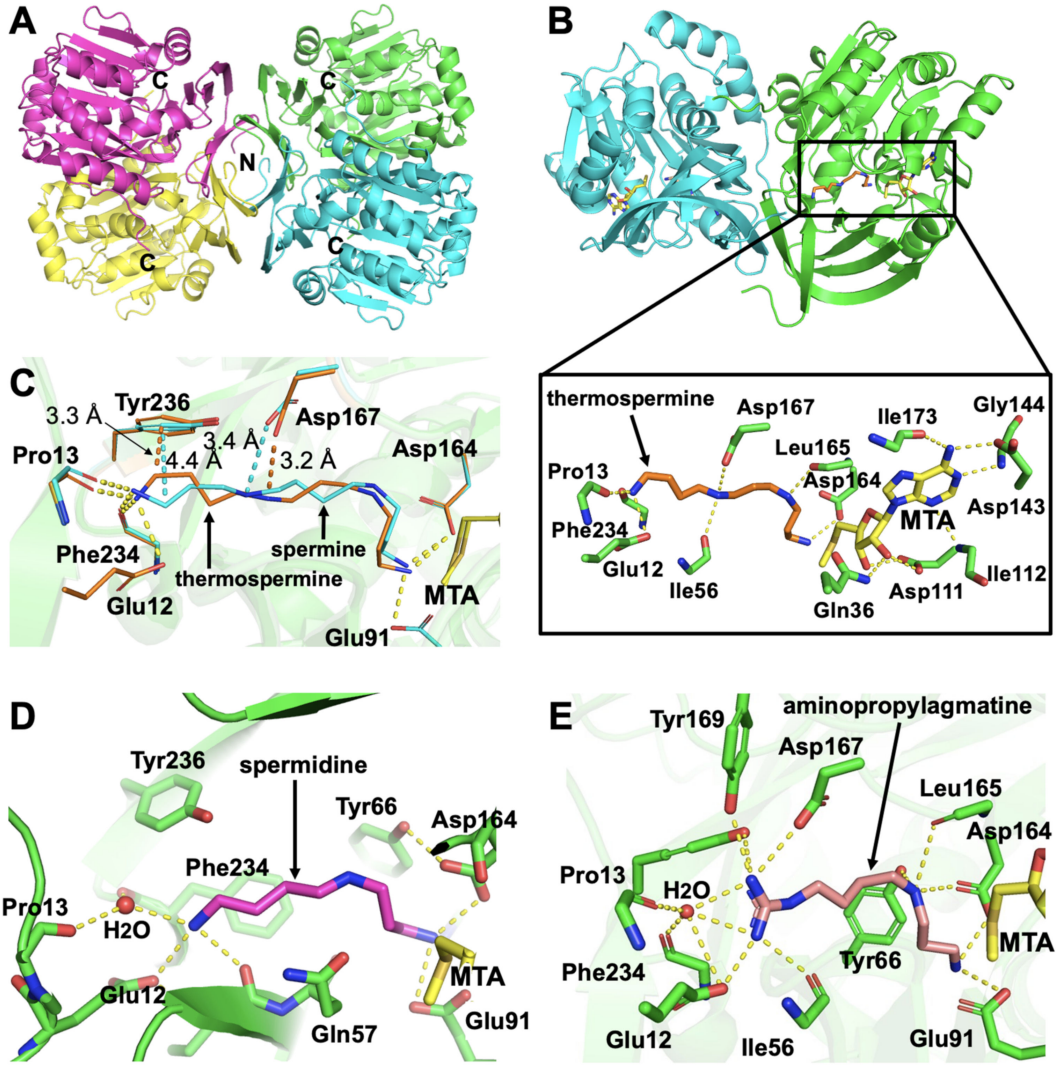

Figure 4. Crystal structures of *Pc*-SpeE. (**A**) The dimer of homodimers (homotetramer) assembly of *Pc*-SpeE. (**B**) The homodimer form of *Pc*-SpeE in complex with MTA and thermospermine (PDB ID: 7XIF). The box indicates the catalytic pocket where ligands bind. (**C**) Structural comparison of the *Pc*-SpeE substrate-binding sites of the MTA and thermospermine complex (7XIF) and the MTA and spermine complex (7XIG). (**D**) Substrate-binding site of *Pc*-SpeE in complex with MTA and spermidine (7XIH). (**E**) Substrate-binding site of *Pc*-SpeE complexed with MTA and aminopropylagmatine (7XII).

The *Pc*-SpeE complexed with MTA and spermidine was obtained by co-crystallization of the protein with dcSAM and putrescine, and the structure (*Pc*-SpeE/MTA/spermidine) was refined to 1.20 Å resolution (Figure 4D). The structure indicated that the catalytic reaction occurred during crystallization and the products generated remained bound in the catalytic pocket. The binding of spermidine was stabilized by interactions with about 10 amino acid residues located within 4.0 Å from spermidine and one water molecule, which was located to accommodate the space created by the shorter spermidine compared with thermospermine/spermine.

The *Pc*-SpeE in complex with MTA and aminopropylagmatine was obtained by co-crystallization of the protein with dcSAM and agmatine, and the structure (*Pc*-SpeE/MTA/aminopropylagmatine) was solved at 2.25 Å resolution (Figure 4E). As anticipated from the kinetic parameters for agmatine (Table 3), the structure shows that the catalytic reaction proceeded during crystallization and the products remained bound in the catalytic pocket. The binding of aminopropylagmatine was stabilized by interactions with about 10 amino acid residues and a water molecule, which existed to fill the space created by aminopropylagmatine being shorter than thermospermine/spermine.

3.4. Polyamine Oxidase Activity and the Polyamine Compositions in P. calidifontis Cells

Archaeal polyamine oxidase-like proteins are found in halophilic archaea [23]. However, no homologous genes of archaeal polyamine oxidase-like proteins were found in the *P. calidifontis* genome. When thermospermine was added to the cell-free extract of *P. calidifontis*, norspermidine was detected in the reaction mixture (Figure 5A). By comparison, almost no 1,3-diaminopropane was produced from spermidine, spermine, or thermospermine in the cell-free extract (data not shown). These results were consistent with the higher K_m and lower V_{max} values observed for *Pc*-SpeE when 1,3-diaminopropane was used as a substrate compared with other substrates (Table 3). Moreover, more norspermidine was formed from thermospermine when electron acceptors (NAD^+, $NADP^+$) were added to the reaction mixture (Figure 5B). When ferricyanide, which was used as the electron acceptor for spermidine dehydrogenase in the in vitro experiment, was added to the polyamine solution, polyamines were degraded nonenzymatically at high temperature (data not shown).

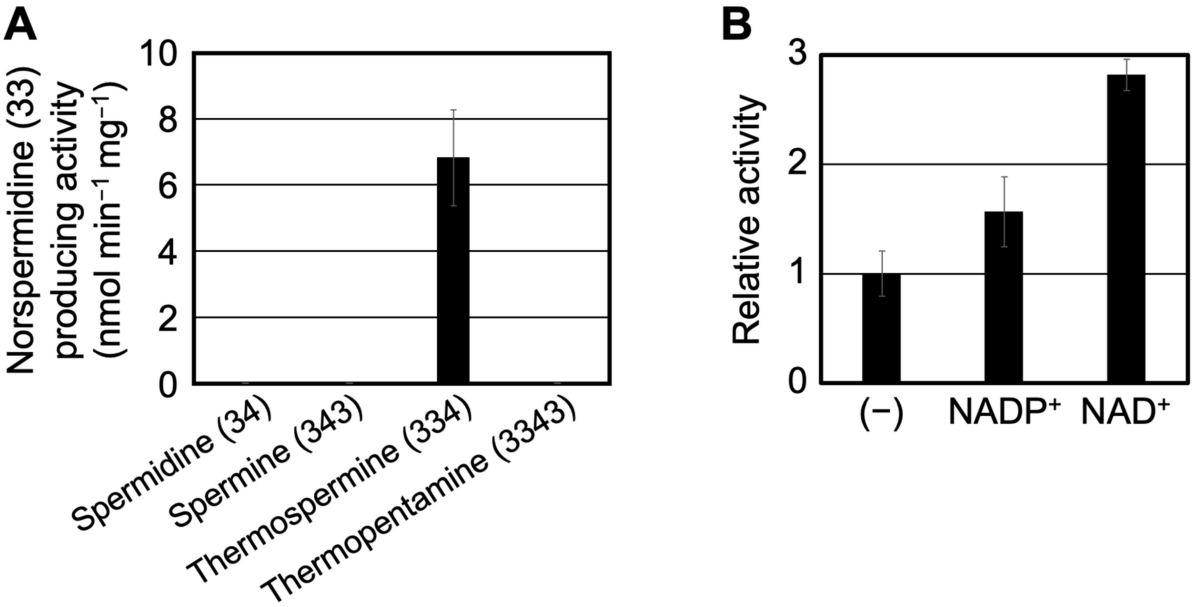

Figure 5. Norspermidine production from polyamines. (**A**) The enzymatic activities of norspermidine production are shown; these were obtained when the polyamines were mixed with a cell-free extract of *P. calidifontis* cultivated under aerobic conditions, followed by incubation at 90 °C for 10 min. (**B**) Norspermidine production from themospermine with electron acceptors. (−) indicates no additional electron acceptors.

When the polyamine composition of *P. calidifontis* cells grown under aerobic or anaerobic conditions were analyzed by HPLC, norspermine was mainly detected regardless of the culture conditions (Figure 2A−C). In addition, small amounts of spermine, norspermidine, and spermine/thermospermine were also detected. A larger amount of spermidine and a smaller amount of spermine/thermospermine were detected from the cells grown under aerobic conditions (Figure 2B,C). An unknown peak (*) observed at a retention time

of 6 min was detected, and the area of the peak decreased under anaerobic conditions (Figure 2A,B). These results suggest that polyamine degradation does not require molecular oxygen. *P. calidifontis* may possess a polyamine dehydrogenase, and polyamines are degraded under anaerobic conditions.

4. Discussion

The aerobic hyperthermophilic archaeon *P. calidifontis* possesses norspermine as a major polyamine in the cell (Figure 2A) [8]. The kinetic parameters obtained for *Pc*-SpeE suggested that agmatine and norspermidine were the major substrates of *Pc*-SpeE (Table 3). Although both thermospermine and spermine could be produced from spermidine, the crystal structure analysis of *Pc*-SpeE suggested that thermospermine was the major product (Figure 4B). Norspermidine was produced via thermospermine or thermopentamine by oxidative degradation. Norspermine, which is the major intracellular polyamine of *P. calidifontis*, is synthesized from norspermidine by the addition of an aminopropyl group. In this pathway, agmatine, spermidine, and norspermidine are substrates of *Pc*-SpeE, and the main chain of these substrates are similar in length. Agmatine is smaller than spermidine and norspermidine; however, aminopropylagmatine with a water molecule was stable in the reaction center of *Pc*-SpeE (Figure 4E). Although *Pc*-SpeE could synthesize thermopentamine in vitro, thermopentamine was not detected in the cell extract [8]. *Pc*-SpeE with spermine as the substrate showed low V_{max} and high K_m values; therefore, the amount of thermopentamine production would be low, and it might be difficult for the large polyamine to be accumulated in the cell. By comparison, a mutant strain of *T. kodakarensis*, which lacks large branched-chain polyamines, was shown to grow at over 90 °C, while the wild type strain grew at even higher temperatures than the mutant strain [4]. Therefore, although large branched-chain polyamines contribute to the growth at high temperatures, large polyamines are not essential for growth at high temperatures.

In archaea, agmatine is used for $tRNA^{Ile}$ modification (agmatidine formation), and agmatine is essential for cell growth [24–26]. Spermidine is synthesized via aminopropylagmatine in thermophiles such as *T. thermophilus* and *T. kodakarensis* [4,27]. *Pa*-SpeE with putrescine as a substrate showed very low activities [18], and *Pc*-SpeE had low affinity for putrescine (Table 3). Considering these results, a polyamine biosynthesis pathway via aminopropylagmatine exists in hyperthermophilic crenarchaea, although the intracellular role of aminopropylagmatine is unknown. By comparison, a small amount of putrescine was detected from other *Pyrobaculum* species such as *P. islandicum* and *P. organotrophum* [8]. Spermidine might be also produced via putrescine in *P. calidifontis*, although the substrate specificity of agmatinase from *P. calidifontis* is still unknown.

The chemical structures of spermidine and norspermidine differ by only one methylene group. However, spermidine tends to align the orientation of DNA, whereas norspermidine induces shrinkage with a greater potency than spermidine [28]. Polyamines stabilize DNA and RNA structure, and spermidine is more effective than norspermidine [29]. Considering norspermidine and norspermine production via spermidine in *P. calidifontis*, polyamines that consist of trimethylene groups between the amine groups may affect gene expression according to the growth phase. Norspermidine was detected from the cells grown under anaerobic conditions. In the case of *P. aeruginosa*, succinate and NADH were produced from 4-aminobutanal produced by spermidine degradation [3]. The respiratory chain of *Pyrobaculum* species contains NADH dehydrogenase and succinate dehydrogenase [30]. The substrates of these respiratory chain dehydrogenases may be produced by polyamine degradation. In fact, NAD^+-dependent thermospermine degradation was detected from the *P. calidifontis* cells (Figure 5B). The identification and characterization of enzymes involved in polyamine degradation in *P. calidifontis* require further study.

5. Conclusions

Although (hyper)thermophilic euryarchaea and bacteria possess long-chain and/or BCPAs, which are especially important for the growth at high temperature, hyperther-

mophilic crenarchaea do not produce BCPAs. In the case of hyperthermophilic crenarchaeon *P. calidifontis*, norspermine (**333**), norspermidine (**33**), and spermidine (**34**) are major intracellular polyamines, but the biosynthesis pathway of these polyamines has been unclear. The enzymatic properties and crystal structures of *Pc*-SpeE suggest that thermospermine (**334**) is mainly produced from arginine via agmatine, aminopropylagmatine, and spermidine. Norspermidine is produced from thermospermine by an unknown polyamine oxidase/dehydrogenase followed by norspermine formation by *Pc*-SpeE.

Author Contributions: Conceptualization, W.F., S.F. and E.M.; biochemical analysis, W.F., M.O., R.H. and S.F.; substrate synthesis for kinetic study, T.H. and N.U.; X-ray crystallography, Y.Y. and E.M.; writing manuscript, W.F. and E.M.; funding acquisition, S.F. and E.M. All authors have read and agreed to the published version of the manuscript.

Funding: This study was mainly supported by a grant from the Japan Society for the Promotion of Science (JSPS) (KAKENHI grant 21H02112). This work was partly supported by a Grant-in-Aid for Scientific Research on Innovative Areas from the Ministry of Education, Culture, Sports, Science, and Technology (MEXT) (19H05780); the Japan Science and Technology Agency (JST), PRESTO (JPMJPR17GB); and a project, JPNP18016, commissioned by the New Energy and Industrial Technology Development Organization (NEDO).

Institutional Review Board Statement: Not applicable.

Informed Consent Statement: Not applicable.

Data Availability Statement: Not applicable.

Acknowledgments: We thank Masaki Kobayashi (Josai Univ.) for GC–MS analysis, and Taku Takahashi (Okayama Univ.) for kindly provision of norspermine. This work was performed using a synchrotron beamline BL44XU at SPring-8 under the Collaborative Research Program of Institute for Protein Research, Osaka University. Diffraction data were collected at the Osaka University beamline BL44XU at SPring-8 (Harima, Japan) (Proposal No. 2018B6850 and 2019B6950).

Conflicts of Interest: The authors declare that they have no conflict of interest.

Abbreviations

dcSAM	decarboxylated *S*-adenosyladenosine
Hb-SpeEI	aminopropyltransferase I from *Hyperthermus butylicus*
Hb-SpeEII	aminopropyltransferase II from *Hyperthermus butylicus*
HPLC	high-performance liquid chromatography
MTA	5′-methylthioadenosine
NAD^+	nicotinamide adenine dinucleotide
$NADP^+$	nicotinamide adenine dinucleotide phosphate
Pa-SpeE	aminopropyltransferase from *Pyrobaculum aerophilum*
Pc-SpeE	aminopropyltransferase from *Pyrobaculum calidifontis*
PDB	Protein Data Bank
PIPES	piperazine-1,4-bis(2-ethanesulfonic acid)
RMSD	root mean square deviation
Tk-BpsA	branched-chain polyamine synthase from *Thermococcus kodakarensis*

References

1. Wang, Y.; Casero, R.A., Jr. Mammalian polyamine catabolism: A therapeutic target, a pathological problem, or both? *J. Biochem.* **2006**, *139*, 17–25. [CrossRef]
2. Janne, J.; Alhonen, L.; Keinanen, T.A.; Pietila, M.; Uimari, A.; Pirinen, E.; Hyvonen, M.T.; Jarvinen, A. Animal disease models generated by genetic engineering of polyamine metabolism. *J. Cell. Mol. Med.* **2005**, *9*, 865–882. [CrossRef] [PubMed]
3. Dasu, V.V.; Nakada, Y.; Ohnishi-Kameyama, M.; Kimura, K.; Itoh, Y. Characterization and a role of *Pseudomonas aeruginosa* spermidine dehydrogenase in polyamine catabolism. *Microbiology* **2006**, *152*, 2265–2272. [CrossRef] [PubMed]
4. Okada, K.; Hidese, R.; Fukuda, W.; Niitsu, M.; Takao, K.; Horai, Y.; Umezawa, N.; Higuchi, T.; Oshima, T.; Yoshikawa, Y.; et al. Identification of a novel aminopropyltransferase involved in the synthesis of branched-chain polyamines in hyperthermophiles. *J. Bacteriol.* **2014**, *196*, 1866–1876. [CrossRef] [PubMed]

5. Fukuda, W.; Yamori, Y.; Hamakawa, M.; Osaki, M.; Fukuda, M.; Hidese, R.; Kanesaki, Y.; Okamoto-Kainuma, A.; Kato, S.; Fujiwara, S. Genes regulated by branched-chain polyamine in the hyperthermophilic archaeon *Thermococcus kodakarensis*. *Amino Acids* **2020**, *52*, 287–299. [CrossRef]
6. Yamori, Y.; Hamakawa, M.; Hidese, R.; Fukuda, M.; Atomi, H.; Fukuda, W.; Fujiwara, S. Branched-chain polyamine stabilizes RNA polymerase at elevated temperatures in hyperthermophiles. *Amino Acids* **2020**, *52*, 275–285. [CrossRef]
7. Oshima, T. Enigmas of biosyntheses of unusual polyamines in an extreme thermophile, *Thermus thermophilus*. *Plant. Physiol. Biochem.* **2010**, *48*, 521–526. [CrossRef]
8. Hamana, K.; Hosoya, R.; Itoh, T. Polyamine analysis of methanogens, thermophiles and extreme halophiles belonging to the domain Archaea. *J. Jpn. Soc. Extrem.* **2007**, *6*, 25–31. [CrossRef]
9. Amo, T.; Paje, M.L.; Inagaki, A.; Ezaki, S.; Atomi, H.; Imanaka, T. *Pyrobaculum calidifontis* sp. nov., a novel hyperthermophilic archaeon that grows in atmospheric air. *Archaea* **2002**, *1*, 113–121. [CrossRef]
10. Amo, T.; Atomi, H.; Imanaka, T. Unique presence of a manganese catalase in a hyperthermophilic archaeon, *Pyrobaculum calidifontis* VA1. *J. Bacteriol.* **2002**, *184*, 3305–3312. [CrossRef]
11. Giles, T.N.; Graham, D.E. Crenarchaeal arginine decarboxylase evolved from an *S*-adenosylmethionine decarboxylase enzyme. *J. Biol. Chem.* **2008**, *283*, 25829–25838. [CrossRef]
12. Sambrook, J.; Russell, D.W. (Eds.) *Molecular Cloning: A Laboratory Manual*, 3rd ed.; Cold Spring Harbor Laboratory Press: New York, NY, USA, 2001.
13. Kabsch, W. XDS. *Acta Crystallogr. Sect. D Biol. Crystallogr.* **2010**, *66*, 125–132. [CrossRef]
14. Winn, M.D.; Ballard, C.C.; Cowtan, K.D.; Dodson, E.J.; Emsley, P.; Evans, P.R.; Keegan, R.M.; Krissinel, E.B.; Leslie, A.G.; McCoy, A.; et al. Overview of the CCP4 suite and current developments. *Acta Crystallogr. Sect. D Biol. Crystallogr.* **2011**, *67*, 235–242. [CrossRef]
15. Vagin, A.; Teplyakov, A. Molecular replacement with MOLREP. *Acta Crystallogr. Sect. D Biol. Crystallogr.* **2010**, *66*, 22–25. [CrossRef]
16. Murshudov, G.N.; Skubak, P.; Lebedev, A.A.; Pannu, N.S.; Steiner, R.A.; Nicholls, R.A.; Winn, M.D.; Long, F.; Vagin, A.A. REFMAC5 for the refinement of macromolecular crystal structures. *Acta Crystallogr. Sect. D Biol. Crystallogr.* **2011**, *67*, 355–367. [CrossRef]
17. Emsley, P.; Lohkamp, B.; Scott, W.G.; Cowtan, K. Features and development of Coot. *Acta Crystallogr. Sect. D Biol. Crystallogr.* **2010**, *66*, 486–501. [CrossRef]
18. Knott, J.M. Biosynthesis of long-chain polyamines by crenarchaeal polyamine synthases from *Hyperthermus butylicus* and *Pyrobaculum aerophilum*. *FEBS Lett.* **2009**, *583*, 3519–3524. [CrossRef]
19. Minguet, E.G.; Vera-Sirera, F.; Marina, A.; Carbonell, J.; Blazquez, M.A. Evolutionary diversification in polyamine biosynthesis. *Mol. Biol. Evol.* **2008**, *25*, 2119–2128. [CrossRef]
20. Ohnuma, M.; Ganbe, T.; Terui, Y.; Niitsu, M.; Sato, T.; Tanaka, N.; Tamakoshi, M.; Samejima, K.; Kumasaka, T.; Oshima, T. Crystal structures and enzymatic properties of a triamine/agmatine aminopropyltransferase from *Thermus thermophilus*. *J. Mol. Biol.* **2011**, *408*, 971–986. [CrossRef]
21. Guedez, G.; Pothipongsa, A.; Siren, S.; Liljeblad, A.; Jantaro, S.; Incharoensakdi, A.; Salminen, T.A. Crystal structure of dimeric *Synechococcus spermidine* synthase with bound polyamine substrate and product. *Biochem. J.* **2019**, *476*, 1009–1020. [CrossRef]
22. Secula, B.; Dauter, Z. Crystal structure of thermospermine synthase from Medicago truncatula and substrate discriminatory features of plant aminopropyltransferases. *Biochem. J.* **2018**, *475*, 789–802. [CrossRef] [PubMed]
23. Salvi, D.; Tavladoraki, P. The tree of life of polyamine oxidases. *Sci. Rep.* **2020**, *10*, 17858. [CrossRef] [PubMed]
24. Ikeuchi, Y.; Kimura, S.; Numata, T.; Nakamura, D.; Yokogawa, T.; Ogata, T.; Wada, T.; Suzuki, T. Agmatine-conjugated cytidine in a tRNA anticodon is essential for AUA decoding in archaea. *Nat. Chem. Biol.* **2010**, *6*, 277–282. [CrossRef] [PubMed]
25. Suzuki, T.; Numata, T. Convergent evolution of AUA decoding in bacteria and archaea. *RNA Biol.* **2014**, *11*, 1586–1596. [CrossRef]
26. Fukuda, W.; Morimoto, N.; Imanaka, T.; Fujiwara, S. Agmatine is essential for the cell growth of *Thermococcus kodakaraensis*. *FEMS Microbiol. Lett.* **2008**, *287*, 113–120. [CrossRef]
27. Ohnuma, M.; Terui, Y.; Tamakoshi, M.; Mitome, H.; Niitsu, M.; Samejima, K.; Kawashima, E.; Oshima, T. N^1-aminopropylagmatine, a new polyamine produced as a key intermediate in polyamine biosynthesis of an extreme thermophile, *Thermus thermophilus*. *J. Biol. Chem.* **2005**, *280*, 30073–30082. [CrossRef]
28. Nishio, T.; Yoshikawa, Y.; Shew, C.Y.; Umezawa, N.; Higuchi, T.; Yoshikawa, K. Specific effects of antitumor active norspermidine on the structure and function of DNA. *Sci. Rep.* **2019**, *9*, 14971. [CrossRef]
29. Terui, Y.; Ohnuma, M.; Hiraga, K.; Kawashima, E.; Oshima, T. Stabilization of nucleic acids by unusual polyamines produced by an extreme thermophile, *Thermus thermophilus*. *Biochem. J.* **2005**, *388*, 427–433. [CrossRef]
30. Nunoura, T.; Sako, Y.; Wakagi, T.; Uchida, A. Regulation of the aerobic respiratory chain in the facultatively aerobic and hyperthermophilic archaeon *Pyrobaculum oguniense*. *Microbiology* **2003**, *149*, 673–688. [CrossRef]